Universiteit Leiden
The Netherlands

A de novo dominant-negative PSMB8 mutation causes severe CANDLE/PRAAS due to arrested proteasome biogenesis

Wolfgramm, S.; Alehashemi, S.; Wendlandt, M.; Thiel, F.G.; Jesus, A.A. de; Papendorf, J.J.; ... ; Goldbach-Mansky, R.

Citation
Wolfgramm, S., Alehashemi, S., Wendlandt, M., Thiel, F. G., Jesus, A. A. de, Papendorf, J. J., ... Goldbach-Mansky, R. (2026). A de novo dominant-negative PSMB8 mutation causes severe CANDLE/PRAAS due to arrested proteasome biogenesis. *Annals Of The Rheumatic Diseases*, *85*(4), 715-729. doi:10.1016/j.ard.2025.10.021

Version: Publisher's Version
License: Creative Commons CC BY 4.0 license
Downloaded from: https://hdl.handle.net/1887/4304799

Note: To cite this publication please use the final published version (if applicable).

Ann Rheum Dis 85 (2026) 715–729

Contents lists available at ScienceDirect

Annals of the Rheumatic Diseases

journal homepage: https://www.sciencedirect.com/journal/annals-of-the-rheumatic-diseases

Autoinflammatory disorders

A de novo dominant-negative *PSMB8* mutation causes severe CANDLE/PRAAS due to arrested proteasome biogenesis

Sophie Wolfgramm[1], Sara Alehashemi[2], Martin Wendlandt[1], Franziska G. Thiel[1], Adriana A. de Jesus[2], Jonas J. Papendorf[1], Hannes Wolfgramm[3], Flavia Llorente Alvarez[1], Emely Borngräber[1], Kat Uss[2], Farzana Bhuyan[2], Anvitha Metpally[2], Leif Steil[3], Christian Hentschker[3], Simone Venz[1], Ruba Al Abdulla[1], Léa Poirier[4], Christopher Friend[2], Fabiola Castello Casta[5], Iren Horkayne-Szakaly[6], Shoghik Akoghlanian[7], Peter J. Mustillo[8], Roshini S. Abraham[9], Paul Bastard[10,11,12,13], Thais C.L. Moura[14], Mayra B. Dorna[14], Katia T. Kozu[14], Jesper Kers[15,16,17], Y. K. Onno Teng[18], Robbert G.M. Bredius[19], Karin Palmblad[20], AnnaCarin Horne[20], Petter Brodin[20], Pilar Blanco-Lobo[21], José Bernabeu-Wittel[21], Laura Fernandez-Silveira[21], Olaf Neth[21], Anne Pagnier[22], Guilaine Boursier[23], Maud Tusseau[24], Thomas W.J. Huizinga[25], Benjamin Fournier[11,13], Bénédicte Neven[11,13], Uwe Völker[3], Gijs W.E. Santen[26], Jason M. Brenchley[5], Katherine R. Calvo[27], David Kleiner[28], Frédéric Ebstein[1,4], Elke Krüger[1,*], Raphaela Goldbach-Mansky[2,**]

[1] *Institute of Medical Biochemistry and Molecular Biology, University Medicine Greifswald, Greifswald, Germany*
[2] *Translational Autoinflammatory Diseases Section (TADS), Laboratory of Clinical Immunology and Microbiology, National Institute of Allergy and Infectious Diseases, National Institutes of Health, Bethesda, MD, USA*
[3] *Department of Functional Genomics, University Medicine Greifswald, Greifswald, Germany*
[4] *Nantes Université, CNRS, INSERM, L'Institut du Thorax, 44000 Nantes, France*
[5] *Barrier Immunity Section, Laboratory of Viral Diseases, National Institute of Allergy and Infectious Diseases, National Institutes of Health Bethesda, MD, USA*
[6] *Joint Pathology Center, Silver Spring, MD, USA*
[7] *Division of Rheumatology, Department of Pediatrics, Nationwide Children's Hospital, Columbus, OH, USA*
[8] *Division of Allergy and Immunology, Department of Pediatrics, Nationwide Children's Hospital, Columbus, OH, USA*
[9] *Department of Pathology and Laboratory Medicine, Nationwide Children's Hospital, Columbus, OH, USA*
[10] *Laboratory of Human Genetics of Infectious Diseases, Necker Branch, INSERM U1163, Necker Hospital for Sick Children, Paris, France*
[11] *University Paris Cité, Institut des Maladies Génétiques (Imagine) Institute, Paris, France*

*Correspondence to Dr. Elke Krüger, Institute of Medical Biochemistry and Molecular Biology, University Medicine Greifswald, Greifswald, Germany.
**Correspondence to Dr. Raphaela Goldbach-Mansky, Translational Autoinflammatory Diseases Section (TADS), National Institute of Allergy and Infectious Diseases, NIH, Bethesda, MD, USA.
E-mail addresses: elke.krueger@uni-greifswald.de (E. Krüger), raphaela.goldbach-mansky@nih.gov (R. Goldbach-Mansky).
Sophie Wolfgramm and Sara Alehashemi contributed equally.
Handling editor Josef S. Smolen.

https://doi.org/10.1016/j.ard.2025.10.021

0003-4967/© 2025 The Author(s). Published by Elsevier B.V. on behalf of European Alliance of Associations for Rheumatology (EULAR). This is an open access article under the CC BY license (http://creativecommons.org/licenses/by/4.0/)

[12] St. Giles Laboratory of Human Genetics of Infectious Diseases, Rockefeller Branch, The Rockefeller University, New York, NY, USA
[13] Pediatric Hematology-Immunology and Rheumatology Unit, Necker Hospital for Sick Children, Assistance Publique-Hôpitaux de Paris (AP-HP), Paris, France
[14] Children's Hospital of the University of Sao Paulo, Sao Paulo, Brazil
[15] Department of Pathology, Leiden University Medical Center, Leiden, Netherlands
[16] Department of Pathology, Erasmus Medical Center, Rotterdam, Netherlands
[17] Department of Pathology, Amsterdam University Medical Center, Amsterdam, Netherlands
[18] Center of expertise for Lupus-, Vasculitis- and Complement-Associated Systemic Autoimmune Diseases, Department of Internal Medicine, Section of Nephrology, Leiden University Medical Center, Leiden, Netherlands
[19] Department of Pediatrics, Leiden University Medical Center, Leiden, Netherlands
[20] Karolinska University Hospital, Stockholm, Sweden
[21] Hospital Universitario Virgen del Rocío, Instituto de Biomedicina de Sevilla (IBiS), CSIC/Universidad de Sevilla, Seville, Spain
[22] French National Reference Center of Autoinflammatory Diseases and Amyloidosis (CeRéMAIA), Immuno-Hémato-Oncologie (IHO), Grenoble Alpes University-Hospital, Grenoble, France
[23] French National Reference Center of Autoinflammatory Diseases and Amyloidosis (CeRéMAIA), CHU Montpellier, Department of Molecular Genetics and Cytogenomics, IRMB, INSERM U1183, Univ Montpellier, Montpellier, France
[24] University Hospital of Lyon, Department of Medical Genetics, CIRI, Inserm U1111, University Claude Bernard Lyon 1, UMR5308, ENS de Lyon, Lyon, France
[25] Department of Rheumatology, Leiden University Medical Center, Leiden, Netherlands
[26] Department of Clinical Genetics, Leiden University Medical Center, Leiden, Netherlands
[27] Hematology Section, Department of Laboratory Medicine, Clinical Center, NIH, Bethesda, MD, USA
[28] Laboratory of Pathology Center for Cancer Research, National Cancer Institute, National Institutes of Health, Bethesda, MD, USA

ARTICLE INFO

Article history:
Received 24 July 2025
Received in revised form 17 October 2025
Accepted 19 October 2025

ABSTRACT

Objectives: Proteasome-associated autoinflammatory syndromes (PRAAS) include a group of autoinflammatory interferonopathies caused by 20S proteasome dysfunction. We characterised pathomechanisms and treatment responses of patients with a de novo, dominant-negative (DN)-proteasome subunit beta type-8 (*PSMB8*) variant.
Methods: Patients with the DN-*PSMB8* p.G209R variant encoding a mutant β5i subunit of the 20S immunoproteasome were evaluated. Interferon biomarkers, proteasome activity, structural modelling, and proteotoxic stress responses were assessed. Patients' T cells underwent integrated transcriptomic and proteomic profiling to characterise immune dysregulation, proteotoxic stress responses, mitochondrial function, and type I interferon (IFN-I) associated stress signalling.
Results: Patients with DN-PRAAS presented with early-onset systemic inflammation, panniculitis, cytopenias, infections, and porto-sinusoidal vascular liver disease (PSVD), indicating broader immune dysfunction that partially responds to Janus kinase inhibition and/or interferon-α/β receptor blockade (anifrolumab). Mechanistically, the *PSMB8* p.G209R variant caused steric hindrance that impaired β5i propeptide processing and final 20S proteasome formation, resulting in intracellular protein aggregation, impaired mitochondrial metabolism, and altered neutral lipid processing. The IFN-I signature of patients' T cells was reduced by blockade of 2 integrated stress response (ISR)-regulating kinases, protein kinase R (PKR) and general control nonderepressible 2 (GCN2), and by Janus kinase signalling.
Conclusions: The DN-*PSMB8* p.G209R variant broadens the clinical and mechanistic PRAAS spectrum by causing 20S proteasome maturation arrest and uncovering a convergence between mitochondrial dysfunction and the ISR. Our findings implicate cytopenia in a pattern of vascular pathology, including PSVD of the liver. We further identify PKR and GCN2 as key mediators of maladaptive IFN-I responses and potential therapeutic targets.

INTRODUCTION

The discovery of loss-of-function (LOF) mutations in proteasome genes as a cause of the autoinflammatory disease spectrum of proteasome-associated autoinflammatory syndromes (PRAAS) has linked the 20S proteasome dysfunction to type I interferon (IFN-I)-driven autoinflammation and spurred investigations into mechanisms connecting impaired proteasome function with chronic inflammation and immune dysregulation, including aberrant IFN-I production [1]. The ubiquitin-proteasome system (UPS) is the principal pathway for degrading misfolded, damaged, or regulatory proteins, thereby maintaining protein homeostasis. In addition to proteolysis, the UPS intersects with a broad spectrum of cellular and metabolic pathways, including autophagy and lysosomal degradation [2–4], nutrient sensing [5,6], lipid metabolism [7], mitochondrial function [8], and immune signalling [9]. Mechanistically, the standard 26S proteasome consists of a 20S core particle with catalytic β1, β2, and β5 subunits, and 1 or 2 19S regulatory particle (s) (RP) for substrate recognition and unfolding, with the latter

WHAT IS ALREADY KNOWN ON THIS TOPIC

- Proteasome-associated autoinflammatory syndromes (PRAAS) are predominantly autosomal recessive diseases caused by variants in immuno- or standard-proteasome subunit genes with type I interferon (IFN-I)-driven autoinflammation that is responsive to Janus kinase inhibition.
- PRAAS is associated with proteotoxic cell stress due to reduced peptide hydrolysis of the 20S proteasome with increased IFN-I signalling dependent on the upregulation of the integrated stress response kinase PKR.

WHAT THIS STUDY ADDS

- Compared to homozygous or compound heterozygous (biallelic) PRAAS, 8 unrelated patients with the first dominant-negative (DN)-proteasome subunit beta type-8 (*PSMB8*) variant presented with broader immune dysregulation, including cytopenias, infections, and porto-sinusoidal vascular liver disease (PSVD), and may require baricitinib and anifrolumab to improve inflammatory control.
- Different cell models and structural modelling uncover the pathomechanism of the DN effect of the *PSMB8* p.G209R variant that results in steric hindrance and stalled propeptide processing at the preholo-proteasome stage that affects ~75% of all 20S immunoproteasomes.
- Molecular profiling of patients' expanded T cells reveals elevated mitochondrial stress and impaired lipid metabolism in DN-PRAAS, likely contributing to T cell dysfunction and cytopenias, which are associated with increased viral susceptibility and the development of PSVD, and contrasts with the milder phenotype observed in biallelic *PSMB8* CANDLE/PRAAS.
- Functional inhibition studies identify GCN2, another serine/threonine kinase that, in concert with PKR, modifies the integrated stress response and IFN-I signalling. Accumulation of intracellular protein aggregates, expansion of exhausted $CD8^+$ T cells, a mitochondrial stress signature, and lipid droplet formation may serve as additional biomarkers, beyond the IFN-I signature, to identify patients at risk for immunodeficiency and PSVD, and to guide treatment stratification.

HOW THIS STUDY MIGHT AFFECT RESEARCH, PRACTICE OR POLICY

- The study identifies a novel pathogenic variant causing DN-PRAAS with immune dysregulation and immunodeficiency, highlights the role of proteasome dysfunction in driving both PSVD and immune impairment, expands the spectrum of therapeutic targets, and proposes a tailored treatment approach within the broader CANDLE/PRAAS continuum.

targeting polyubiquitylated proteins [10,11]. The immunoproteasome, a specialised proteasome complex, is defined by the high-efficiency inducible catalytic subunits, β1i, β2i, and β5i, encoded by (*PSMB10*), *PSMB9,* and (*PSMB8*), that emerged following the genome-wide duplication ~500 million years ago, at the beginning of vertebrate diversification and adaptive immunity evolution [12]. It enhances antigen presentation and provides protection during IFN-induced oxidative stress and cytokine exposure [9,13–15]. The immunoproteasome subunits are upregulated in immune and nonimmune cells in response to IFNs and depend on the proper assembly involving proteasome maturation protein (POMP) and other chaperones [16–19].

LOF variants in 20S proteasome subunits underlie the spectrum of PRAAS, originally described in Hispanic [20,21] and Japanese [22,23] founder populations with *PSMB8* variants causing the same disease that is referred to as NNS: Nakajo-Nishimura syndrome; JASL: Japanese autoinflammatory syndrome with lipodystrophy, or CANDLE: chronic atypical neutrophilic dermatosis with lipodystrophy and elevated temperature [24]. Later discoveries of variants in genes encoding other 20S subunits (eg, proteasome subunit alpha type-3 (*PSMA3*), *PSMA5, PSMB4, PSMB9, PSMB10*) [25–32] and assembly chaperones (eg, *POMP* and proteasome assembly chaperone 2 (*PSMG2*)) [26,33–35] have expanded the clinical spectrum to include immunodeficiencies and infections. These range from recessive homozygous or (compound) heterozygous *PSMB8* variants [20,22–26,36–45] and DN variants including *POMP, PSMB9,* and *PSMB10,* the latter presenting with more prominent features of immunodeficiency [26,29–33,35]. CANDLE/PRAAS patients typically exhibit a prominent IFN-I signature [46], and the robust clinical response to Janus kinase inhibitors (JAKi), which block IFN signalling, provides clinical validation of a central role of IFN in driving inflammatory disease manifestations [47]. However, prolonged or high-dose JAKi treatment can lead to infections, including viral reactivation, which is particularly concerning in patients with more severe immune dysregulation. Recent studies have identified a role of the integrated stress response (ISR) serine/threonine kinase, protein kinase R (PKR), as sensor of proteotoxic stress through binding to misfolded indicator protein, interleukin 24 (IL-24), and activation of IFNβ signalling [48]; however, integration with other proteasome-mediated cell stress responses including mitochondrial dysfunction and metabolic dysregulation and their impact on organ dysfunction and damage are not well understood.

We report the first de novo *PSMB8* variant, p.G209R, that causes a dominant-negative (DN)-PRAAS phenotype with clinical features of immune dysregulation, which is not seen in CANDLE patients with disease-causing biallelic *PSMB8* variants. Through structural modelling and cellular profiling, we characterise mitochondrial and metabolic lipid stress, in addition to intracellular protein aggregates in patients' T cells, and thus expand the characterisation of maladaptive cell stress responses that contribute to immune dysregulation and provide novel treatment targets.

MATERIALS AND METHODS

Ethic statement

Patients 1 to 7 and healthy donors (HDs) were enrolled in the Natural History, Pathogenesis, and Outcomes of Autoinflammatory Diseases protocol (NCT02974595) at the National Institutes of Health (NIH), in Bethesda, MD, USA, with written informed consent obtained from participants or their legal guardians. Buffy coats from HDs and previously published HDs [49] were obtained for some experiments under protocol (BB 209/18 and BB 014/14). Patient 8 was enrolled at Imagine Institute, France (IRB number: 22.00729.000060).

Patient studies

DN patients were clinically assessed, and genetic analysis, clinical biomarkers assessment, including IFN signature and response to JAKi, and IFNAR blockade. Expanded T cells were generated from DN-PRAAS patients (Pt 1, Pt 2, Pt 4 and Pt 8), biallelic *PSMB8* (β5i) CANDLE/PRAAS patients, and from HDs (see Supplementary Methods).

Additional methods and materials can be found in the Supplementary Methods.

RESULTS

Clinical description

Through international collaboration, the cohort included 8 patients (5 female), aged 2 to 30 years, who all harbour a heterozygous *PSMB8* p.Gly209Arg (G209R) variant (6/8 de novo, 2/8 assumed de novo). Disease onset occurred in the neonatal period, and in 7/8 presented with fever, rash, and systemic inflammation (Fig 1A-F; S1 A-C). Patient 1 died at age 25 years from complications of portal hypertension, in the context of nodular regenerative hyperplasia (NRH). Patient 3 passed away at the age of 5 years due to cytomegalovirus (CMV) pneumonia. The clinical description of the cohort is summarised in Table S1.

Compared to patients with biallelic or digenic PRAAS, infections were frequent in all patients from an early age, including pneumonia and sepsis. Hepatosplenomegaly, abdominal distention, and ascites were common (7/8). Two patients were also diagnosed with congenital thyroid gland agenesis in infancy (Fig 1F, Table S1). The clinical characteristics of the DN cohort, including cytopenias, infections, and organ involvement, are depicted in comparison to biallelic PRAAS in Figure 1F. Haematologic and immunologic abnormalities were prominent in the cohort. Anaemia was observed in all patients (8/8), while persistent lymphopenia and hypogammaglobulinemia were observed in 7 out of 8 patients, who were all placed on immunoglobulin replacement therapy. Thrombocytopenia in 6 patients with splenomegaly was suggestive of splenic sequestration. Serial bone marrow biopsies (patient 2) showed variable hypocellularity, ranging from approximately 20% during systemic viral infection, to 60% −70% on treatment with anifrolumab and JAKi. The biopsies demonstrated preserved trilineage hematopoiesis, a marked reduction in B-cell lymphoid precursors, and preserved or increased myeloid cells. Flow analysis showed normal neutrophil maturation. (Fig S2). $CD4^+$, $CD8^+$ T-cell, and $CD19^+$ B-cell counts in the peripheral blood were plotted as a function of age. In comparison to age-matched controls, $CD19^+$ B cell lymphopenia with borderline $CD4^+$ T cell lymphopenia was documented and was lower in DN patients compared with digenic and biallelic *PSMB8* CANDLE patients. (Fig S3). Early in life, transient increases in CD19 counts and $CD4^+$ and $CD8^+$ T cells following documented viral infections suggested appropriate bone marrow responses (Fig 1G). Seven out of 8 patients had elevated acute phase reactants, and all had elevated IFN-I scores supporting an interferon-driven inflammatory process (Fig 1H and Supplementary Methods). All patients (8/8) experienced recurrent infections. Viral infections (8/8) included Epstein-Barr virus, CMV, norovirus, adenovirus, rotavirus, rhinovirus, coronavirus, parainfluenza, human herpesvirus 6, and human herpesvirus 8. Bacterial infections (5/8) included *Pneumocystis jirovecii* pneumonia (n = 2), *Pseudomonas aeruginosa* (n = 2), pneumococcal pneumonia (n = 1), and *Mycoplasma pneumoniae* (n = 1). Fungal infections (3/8) comprised pulmonary aspergillosis and cutaneous candidiasis and parasitic infection with *cryptosporidium* (n = 1).

NRH was identified in all patients who underwent liver biopsy (4/4) during the evaluation of transaminitis and hepatosplenomegaly. Serum levels of intestinal fatty acid–binding protein (I-FABP), a marker of gut epithelial damage and increased intestinal permeability, were markedly elevated in 2 patients (3 samples) with the DN-*PSMB8* variant. Patients with digenic PRAAS (2 patients, 4 samples) also showed elevated I-FABP levels, albeit to a lesser extent, whereas levels in biallelic PRAAS patients (3 patients, 4 samples) remained within the normal range (Fig 1I). These findings suggest that increased gut permeability in DN-PRAAS may contribute to bacterial translocation and liver pathology [50].

Seven of 8 patients received systemic corticosteroids (0.2–1 mg/kg/day), and 5 received additional disease-modifying therapies, including hydroxychloroquine (1/5), mycophenolate (3/5), methotrexate (2/5), infliximab (2/5), rituximab (1/5), antithymocyte globulin (1/5), and colchicine (1/5). Responses were partial and transient.

JAK inhibitors were initiated in 5 of 8 patients (3 received tofacitinib and 2 received baricitinib). All JAKi-treated patients demonstrated clinical improvement and discontinued disease-modifying drugs as outlined in Table S1. However, in contrast to biallelic *PSMB8* patients, who show normalisation of type I and type II IFN signatures on baricitinib, DN-PRAAS patients exhibited resolution of cutaneous manifestations and improvement in myositis but only partial normalisation of systemic inflammatory markers and IFN signatures (Fig 1K,L).

Two patients (patient 2 and patient 4) with incomplete responses to JAKis were subsequently treated with anifrolumab, a monoclonal antibody targeting the type I interferon receptor (IFNAR1). Both achieved normalisation of IFN scores (Fig 1J,K) and were able to discontinue systemic corticosteroids and taper high-dose JAKis. However, lymphopenia and susceptibility to recurrent viral infections persisted, and both patients showed progression of liver disease, including worsening splenomegaly and transaminitis.

Discontinuation of JAKi on anifrolumab treatment in 1 patient led to a clinical flare with elevation of C-X-C motif chemokine 9 (CXCL9) and re-emergence of skin lesions that subsided with reinstation of baricitinib (Fig 1J), suggesting that clinically relevant immune dysregulation in DN-CANDLE/PRAAS may extend beyond type I IFN signalling.

Compared with ‘classic PRAAS’ (biallelic *PSMB8* CANDLE/PRAAS), the DN cohort exhibits both overlapping features—such as panniculitis, lipodystrophy, and elevated IFN scores—and unique manifestations, including more pronounced cytopenias, susceptibility to infections, nodular regenerative hyperplasia, and nephropathy (Fig 1L). Patient 2 is currently undergoing evaluation for haematopoietic stem cell transplantation (HSCT) due to chronic *Pseudomonas aeruginosa* infections, early bronchiectasis, and progression of NRH with worsening splenomegaly.

The de novo heterozygous PSMB8 *p.G209R variant is predicted to be pathogenic and causes decreased immunoproteasome formation*

In silico predictions using MetaRNN (scores of 0.9511 and 0.9514) and AlphaMissense prediction (score of 0.842) support the pathogenicity of the *PSMB8/β*5i variant (c.625G>A and c.625G>C), which substitutes glycine with arginine at protein position 209, without predicted splicing impact (SpliceAI <0.2) (Table S2). Unlike the common founder mutation, p.T75M (minor allele frequency (MAF) 0.000025), p.G209R is absent from population databases, further supporting pathogenicity per ACMG/AMP criteria and suggesting a likely DN effect. Patient 4 also harboured 2 inherited *ADRM1* variants, affecting a 19S RP subunit of the 26S proteasome. ACMG predictions were benign and likely benign (Fig 1E, Table S1), and transfected variants had no significant impact on proteasome function. Additional variants observed in individual patients (Table S1) were not

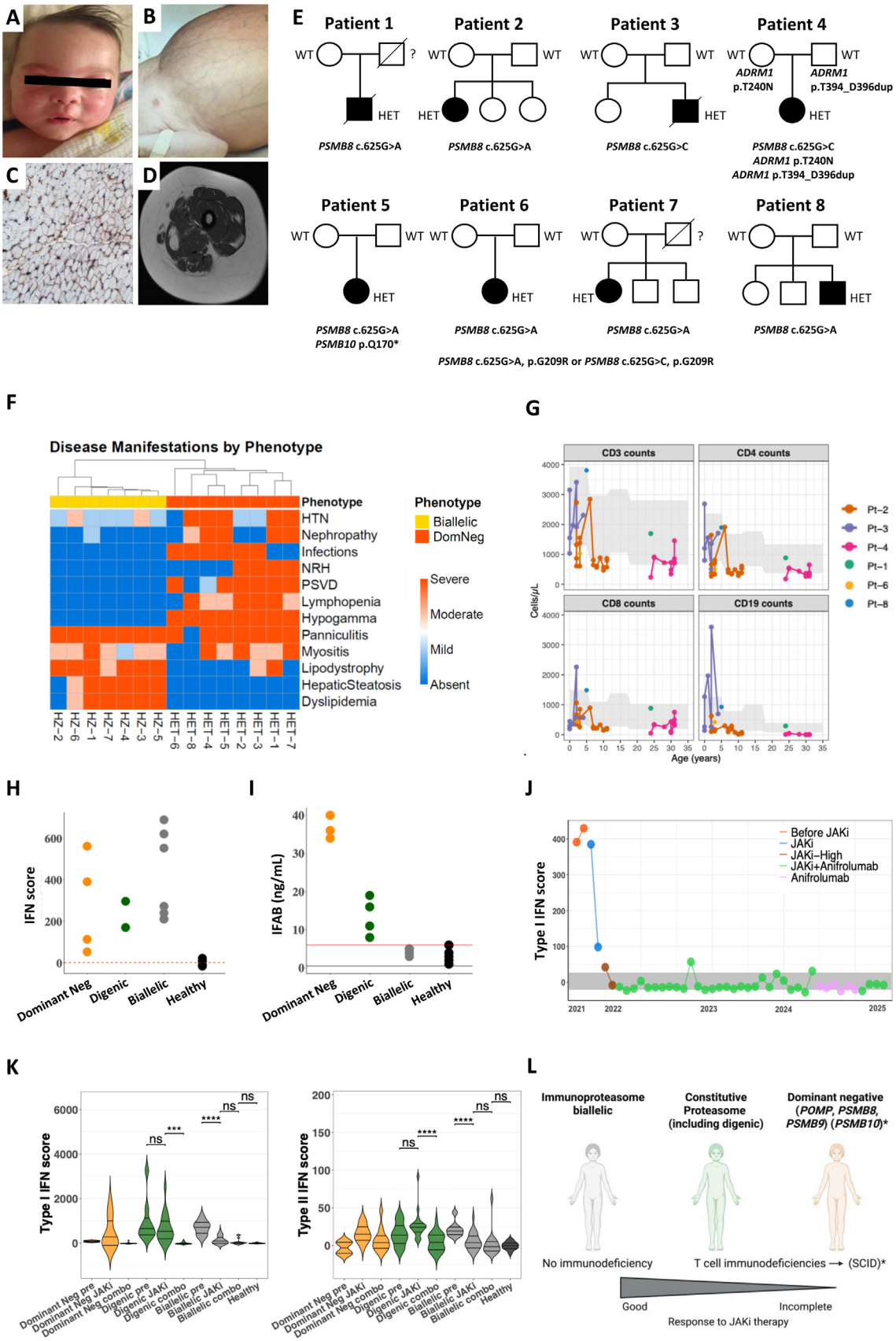

Figure 1. Clinical, histologic, genetic, and biomarker characterisation of patients with dominant-negative *PSMB8* mutations. A–B, Clinical photos showing a violaceous facial rash with periorbital oedema (A) and abdominal distention with prominent abdominal veins, indicative of portal hypertension, ascites, and hepatosplenomegaly (B). C, Muscle biopsy (20 ×) showing diffuse MHC class I upregulation and perifascicular myofibre atrophy, consistent with chronic inflammatory myopathy. D, Axial T1-weighted MRI of the lower extremities showing symmetrical patchy fat replacement and muscle atrophy (left thigh image shown). E, Pedigrees of affected individuals with heterozygous *PSMB8* p.G209R mutations, de novo in most cases. Additional heterozygous proteasome-related variants (*ADRM1* and *PSMB10*) are indicated, whereas proteasome-unrelated variants are mentioned in Table S1. Filled symbols represent affected individuals. Patients 1 and 3 are deceased. F, Heatmap summarizing clinical phenotypes in heterozygous (HET, n = 8) and homozygous (HZ, n = 7) *PSMB8* mutation carriers. Colour intensity reflects severity scores (0–3, absent, mild, moderate, severe)

considered relevant, as the de novo *PSMB8* p.G209R variant was shared across all patients and was selected for in-depth analysis.

To characterise proteasome activity of the *PSMB8* p.G209R variant, we assessed proteasomal chymotrypsin-like activity in expanded T cells from patients and controls in native PAGE assays, which was decreased in proteasome complexes (Fig 2A-D; S4A-D). Total proteasomal activity staining was decreased in proteasome-specific activity-based assessment (Fig S4E), similarly to caspase and trypsin-like activity that were assessed in patient 4 compared to the controls (Fig S4F). Staining of proteasome complexes, α6 and β5i, indicated a partial assembly defect with accumulation of 20S precursor complexes at lower molecular weight (Fig 2D). The decreased β5i signal suggested less incorporation of the mutant subunit into active proteasomes, a finding consistent with haploinsufficiency (Fig 2D; S4A). The staining for 19S cap component, Rpn5, was similar to HDs (Fig S4B), suggesting normal recruitment of the 19S regulatory cap.

Immunoblotting showed higher standard β5 subunit expression than control with unchanged total β5i protein levels (proform and matured form), while incorporation of the other standard catalytic subunits, β1 and β2, and the induced subunits, β1i and β2i, were similar to controls (Fig 2E) suggesting decreased incorporation of the β5i G209R variant into the active proteasome with a partial compensatory replacement by the constitutive β5 subunit accounting for the decreased β5i activity observed. Accumulation of proteasome precursor complexes (Fig 2D, left panel) and increased residual levels of the assembly helper chaperone POMP (Fig 2E, right panel; S4G) indicate that the β5i G209R variant perturbed proteasome assembly, resulting in POMP retention in an incompletely matured proteasome complex.

Transfection studies confirm a proteasome maturation defect caused by the PSMB8 *p.G209R variant*

To study the impact of the *PSMB8* p.G209R variant on proteasome maturation and assembly *in vitro*, we transfected V5-epitope-tagged mutant and wild-type *PSMB8* constructs into C20 microglia cells, EA.hy926 human endothelial cells, and HeLa cells, a human epithelial cell line (Fig 3; S5-7). Two cell lines (C20 and EA.hy926) were CRISPR/Cas9 engineered to lack endogenous *PSMB8*/β5i (*PSMB8* knock out (KO)). V5-epitope-tagged versions of β5i were quantified in immunoblots (Fig 3A-B; S5A-B; S6A-B). Strikingly, in all parental and KO cells transduced with the mutant β5i G209R-V5 construct, the mutant propeptide was not cleaved off completely, suggesting failed propeptide processing for maturation of the subunit (Fig 3B; S5B; S6A). In contrast, the WT construct and the known CANDLE-causing β5i T75M-variant allowed for pro-β5i cleavage and final proteasome maturation, albeit decreased efficiency was seen with β5i T75M-V5 [26].

These data suggest that the p.G209R variant may exert the DN effect by affecting proteasome formation even if WT β5i is endogenously expressed in parental cells. We studied proteasome precursor complexes and identified accumulation of a 20S proteasome intermediate complex in all β5i G209R-V5-expressing cells (Fig 3C; S5C; S6B) that migrates slower and retains the assembly chaperone POMP, which identifies a premature 20S proteasome complex [51] (Fig 3C; S5C). These experiments further indicate that POMP cannot be degraded in the maturation-arrested β5i G209R-mutant proteasome complex. Despite these defects, the cell models do not show striking alterations in the chymotrypsin-like activity (Fig S5E; S6C; S7C).

POMP is required for the incorporation of β5 and β5i; however, β5i has a significantly higher affinity to POMP and is thus preferentially incorporated [18]. Co-immunoprecipitation of FLAG-tagged POMP with wild-type β5i WT-V5 or mutant β5i G209R-V5 showed less association of mutant β5i G209R with POMP compared to the β5i WT-V5 in HeLa cells (Fig 3D; S6D). These results led to the conclusion that a better compensation of proteasome activity by β5 was blocked by β5i G209R mutant interaction with POMP and the incorporation of the mutant variant into nascent proteasome complexes that cannot mature.

The β5i G209R variant blocks conformational changes required for proteasome maturation

To interrogate the structural basis for the proteasome maturation arrest at the preholo-proteasome stage, we used updated structural models of standard 20S-proteasome precursors [51] and immunoproteasomes from various mammalian species, combining available structures with AlphaFold3 predictions for the subunit variant. Proteasome assembly involves multiple steps and chaperones, including POMP and proteasome assembly chaperones (Fig 4A) [19,51]. The glycine at β5i position G209 resides within a compact helix (p.N204 to p.G214) that closely interacts with 2 helices of the opposing β4-subunit, suggesting a critical interface during proteasome biogenesis (Fig 4B,C). Substituting glycine (G) with a bulky, positively charged arginine (R) at p.G209 introduces a steric hindrance, as the arginine side chain clashes with β4 residues T139 and E166,

across 10 clinical domains. HTN, hypertension; NRH, nodular regenerative hyperplasia; PSVD, porto-sinusoidal vascular disease of the liver. G, Age-dependent distribution of $CD3^+$, $CD4^+$, $CD8^+$ T-cell, and $CD19^+$ B cell counts in representative dominant negative CANDLE patients compared with age-appropriate reference ranges (grey shading). Each dot represents a single measurement for an individual subject. Subjects Pt-2, Pt-3, and Pt-4 had longitudinal assessments, and connecting lines trace serial values over time. Subjects with a single available time point, including Pt-1, Pt-6, and Pt-8 are displayed as individual dots. The shaded grey area corresponds to published normative ranges for each lymphocyte subset. H, Type I interferon (IFN) scores measured using a 28-gene panel in HET (n = 5), HZ (n = 2), and biallelic (n = 7) *PSMB8* mutation carriers compared to healthy controls (HC, n = 6). Red lines indicate assay thresholds. I, Circulating intestinal fatty acid binding protein (IFABP) levels in HET (2 patients, 3 samples), digenic (2 patients, 4 samples), biallelic (3 patients, 4 samples), and HC (n = 6). Red lines indicate assay thresholds. J, Longitudinal IFN scores over three years in a patient treated with JAK inhibitor (JAKi) and IFNAR1 blockade with anifrolumab. Initial JAKi monotherapy with baricitinib (0.2 mg/kg) incompletely suppressed the IFN signature, requiring high-dose systemic steroids. Escalation to 0.3 mg/kg daily is limited by recurrent infections. Combination JAKi and anifrolumab therapy achieved durable IFN suppression, enabling baricitinib tapering (0.1 mg/kg daily) and steroid discontinuation. IFNAR1 blockade monotherapy with anifrolumab maintained low IFN scores but was associated with disease flare (rash, myositis, and CXCL9 elevation). Resumption of combination therapy restored remission. K, Type-I and type-II IFN scores by DN (yellow, n = 4 patients), digenic (green, n = 2 patients) and biallelic (grey, n = 9 patients) CANDLE/PRAAS patients before and during JAKi and on JAKi + anifrolumab (combo) therapy compared to controls (black, n = 21 patients). For DN, combo therapy data reflect a single patient. Significant differences were detected for digenic JAKi vs combo (***$P < 0.001$) and biallelic pretreatment vs JAKi (***$P < 0.001$); all other comparisons were not significant (ns). L, Overview of inherited or dominant-negative CANDLE/PRAAS variants and their response to JAKi therapy. Created in BioRender. Venz, S. (2025) https://BioRender.com/ow4aslt.

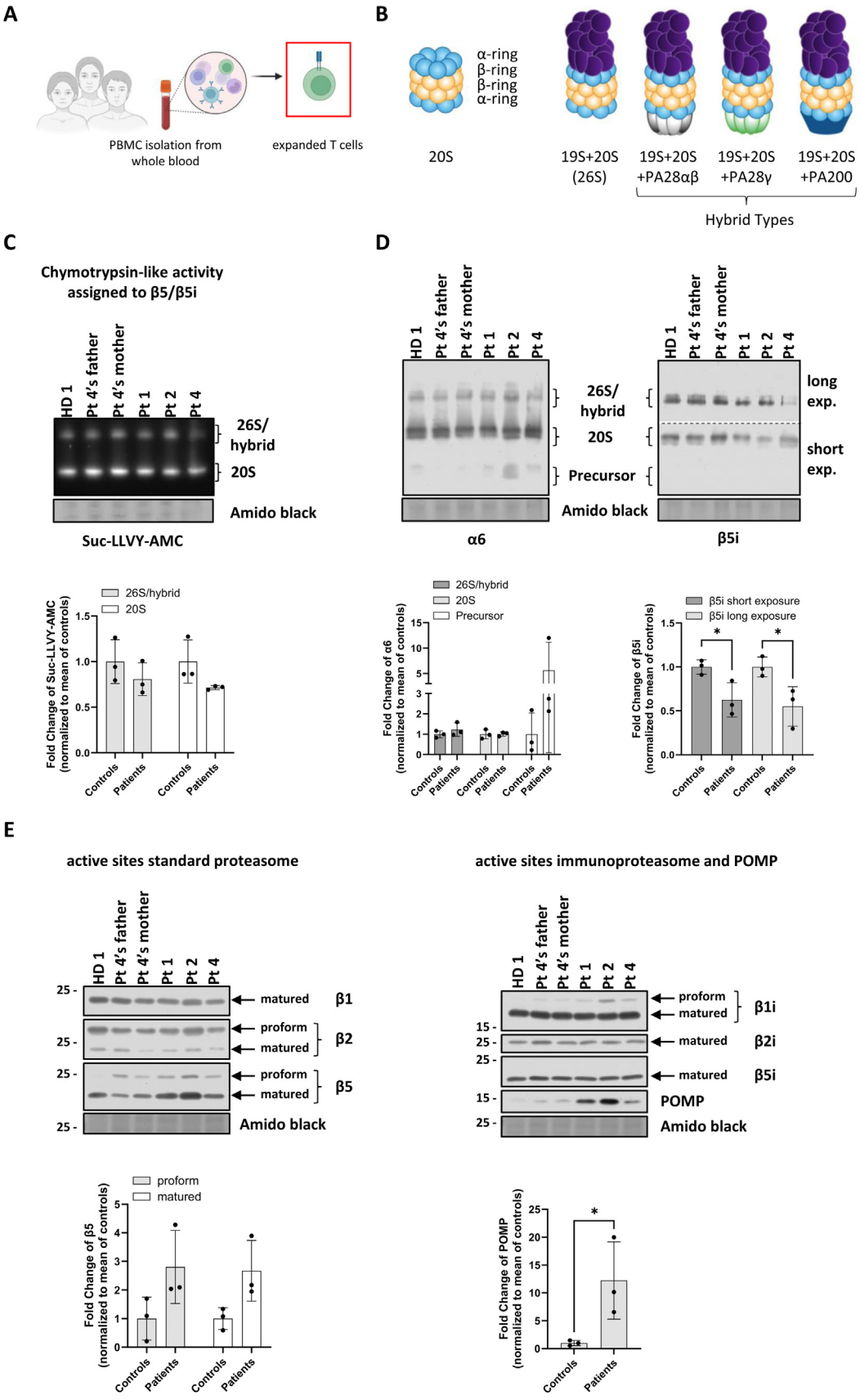

Figure 2. Analyses of proteasome activity and proteasome complexes in patients' expanded T cells. A, Expanded T cells derived from peripheral blood mononuclear cells (PBMCs) from patients and healthy donors were used for analysis. B, Representative illustration of 20S proteasome, 26S proteasome, and hybrid proteasomes. C, In-gel activity assay of chymotrypsin-like activity (Suc-Leu-Leu-Val-Tyr-7-amino-4-methylcoumarin, Suc-LLVY-AMC) and its densitometric analysis from patients 1, 2, and 4 (Pt 1, 2, and 4), including healthy donors: HD 1 and the unaffected parents from patient 4. D, Immunoblots of native PAGE gels and their densitometric analysis from patients 1, 2, and 4 (Pt 1, 2, and 4), including healthy donors: HD 1 and the unaffected parents from patient 4 that were stained with an α6 and β5i antibody to visualise proteasome complexes. The horizontal black dotted line indicates a border to visualise 2 different exposure (exp.) times (long and short) of the same membrane. E, Immunoblots and densitometric analyses showing alterations within the protein expression regarding the catalytically active sites of the standard and immunoproteasomes and the assembly

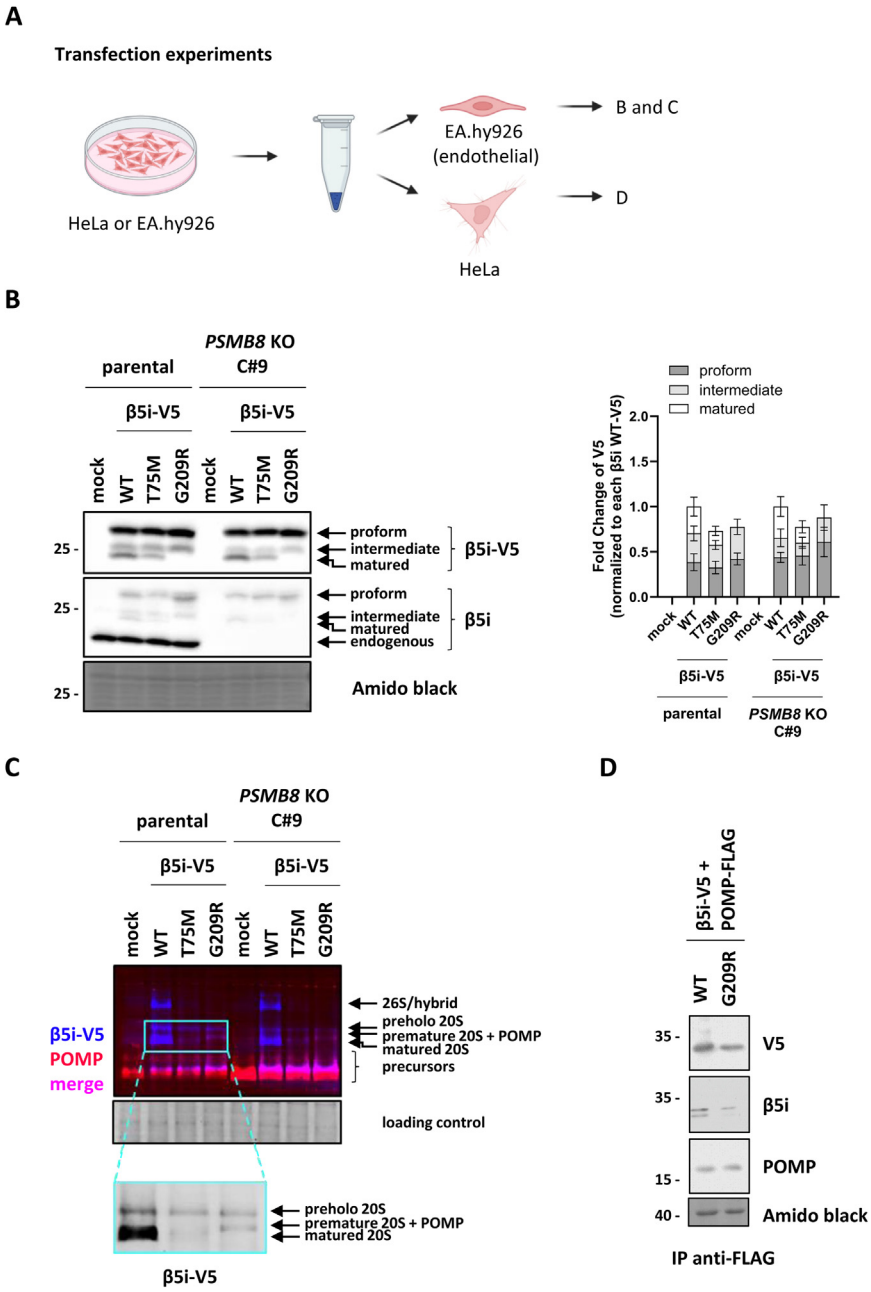

Figure 3. Molecular and functional analyses of EA.hy926 and HeLa *PSMB8*/β5i variants in transfected cells. A, Scheme of cell models used for analysis in B-D. B, SDS-PAGE immunoblot of β5i and V5-tagged β5i in EA.hy926 β5i WT-V5/HIS, β5i T75M-V5/HIS, and β5i G209R-V5/HIS transfected cells depicting the propeptide processing of β5i. Densitometric analysis was performed with n = 5. C, Cofluorescence staining (V5-tagged β5i and POMP) of EA.hy926 β5i WT-V5/HIS, β5i T75M-V5/HIS, and β5i G209R-V5/HIS transfected cells in native PAGE showing different proteasome complexes (n = 3). D, Immunoprecipitation of FLAG-tagged POMP in HeLa transfected β5i WT-V5/HIS and β5i G209R-V5/HIS cells depicting the interaction with β5i (n = 2). Densitometric analysis was normalised to the respective loading control using ImageJ and GraphPad Prism (v.10.2.2). Statistic was applied using the Friedman test with Dunn's correction in GraphPad Prism (v.10.2.2) (Table S3). Created in BioRender. Venz, S. (2025) https://BioRender.com/tsiovsf.

destabilising β4/β5i interactions and preventing proper proteasome maturation (Fig 4C). This likely disrupts the required conformational 'twist' necessary for propeptide processing and final proteasome maturation (Fig 4D), providing a mechanism for the observed maturation defect. Furthermore, the variant perturbs the close approximation of residues within the C-terminal arm of β7/*PSMB4* and the opposing β1/β2 subunits that upon fusion reposition a catalytic lysine triad to activate a catalytic threonine through autocatalysis. The disruption results in β1 propeptide retention [52,53]. This steric clash/hindrance occurs when one or both half-proteasomes incorporate the DN-*PSMB8* variant and thus may affected up to ~75% of immunoproteasomes, consistent with a DN effect (Fig 4E).

Molecular profiling of patient T cells revealed a mitochondrial and metabolic stress signature and an ISR-dependent IFN-signature

The more pronounced cytopenias and T cell-related pathology in the DN-PRAAS patients compared to biallelic PRAAS suggested broader immune dysregulation caused by the β5i G209R-variant, prompting a comparative omics approach to identify cell stress signatures beyond the ISR (Fig 5A). Proteasome

helper POMP of patients 1, 2, and 4 (Pt 1, 2, and 4) to healthy donors, including HD 1 and the unaffected parents from patient 4. Representative Amidoblack stainings show loading and transfer efficiency. All densitometric analyses were normalised to the respective loading controls using ImageJ and GraphPad Prism (v.10.2.2). For statistical testing, an unpaired *t* test was performed, considering a *P* value ≤ 0.05 (*) as significant. Created in BioRender. Venz, S. (2025) https://BioRender.com/jgt88oy; https://BioRender.com/tsiovsf.

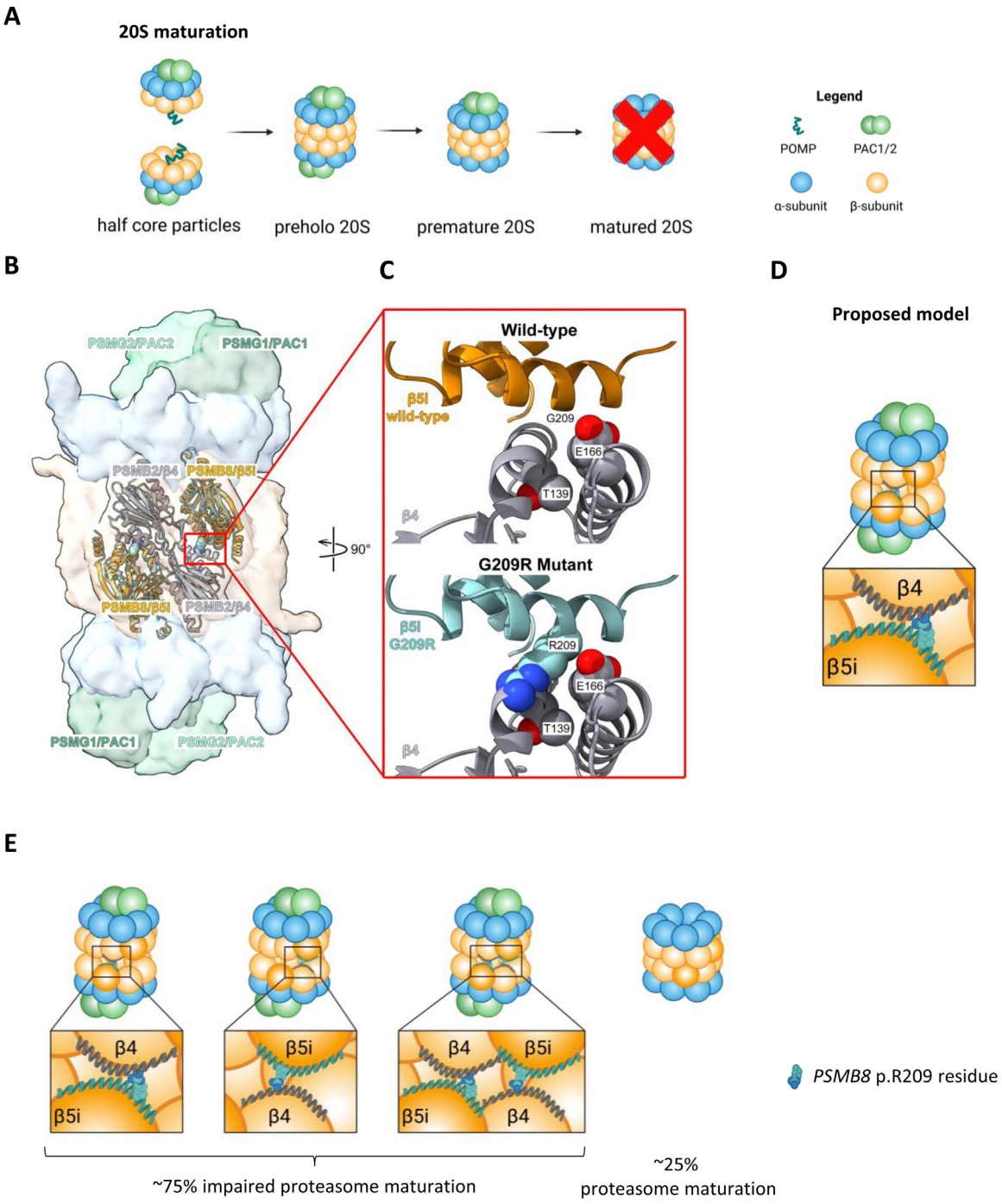

Figure 4. *In silico* steric modelling of de novo PSMB8 Gly209Arg mutation using the preholo-proteasome crystal structure. A, Illustration of the standard 20S maturation. The frame highlights the used structural model for B. B, Cartoon of the standard 20S preholo-proteasome (PDB:8QYS) and the superpositioned β5i (*PSMB8*) with its close interaction side to β4 (*PSMB2*). The red frame indicates the region of interest (C). C, Zoom-in of β5i structure (orange) within the preholo-proteasome, highlighting the variant's position at 209 in the wild-type structure and the closely related amino acids of β4 (grey). The steric clash between the mutated β5i (turquoise) and β4 (grey) is shown by using AlphaFold3 to introduce the amino acid exchange of β5i at position 209 from a glycine (G) to an arginine (R). D, Proposed model of β5i-G209R incorporated proteasomes based on the preholo-proteasome structure, indicating a maturation stop (A). E, Probability of *PSMB8* p.G209R incorporation within the proteasome biogenesis process. Created in BioRender. Venz, S. (2025) https://BioRender.com/s7 × 9ft6; https://BioRender.com/lp7rt0z.

defects can initiate a vicious cycle with mitochondrial impairment, compounding cellular stress [54]. To assess this interplay, we profiled phytohaemagglutinin-lectin (PHA-L) + IL-2 activated T cells (Supplementary Methods), which represent a maximally activated and metabolically stressed state that models immune activation-induced cellular stress. Proteomic and transcriptomic analyses revealed that hallmark cellular and metabolic pathways are more disrupted in DN than biallelic PRAAS T cells, with a prominent cell death signature in DN-PRAAS in transcriptomic (Fig S8A) and proteomic profiling (Fig S9A). Proteomic profiling suggested mitochondrial dysfunction and related metabolic pathways in CANDLE/PRAAS compared to controls (Fig S9A). Activated T cells from both DN and biallelic *PSMB8* PRAAS patients showed protein signatures of impaired mitochondrial respiration (reduced COX5B, SYNE2, AK4), but only DN-PRAAS T cells downregulated proteins critical for

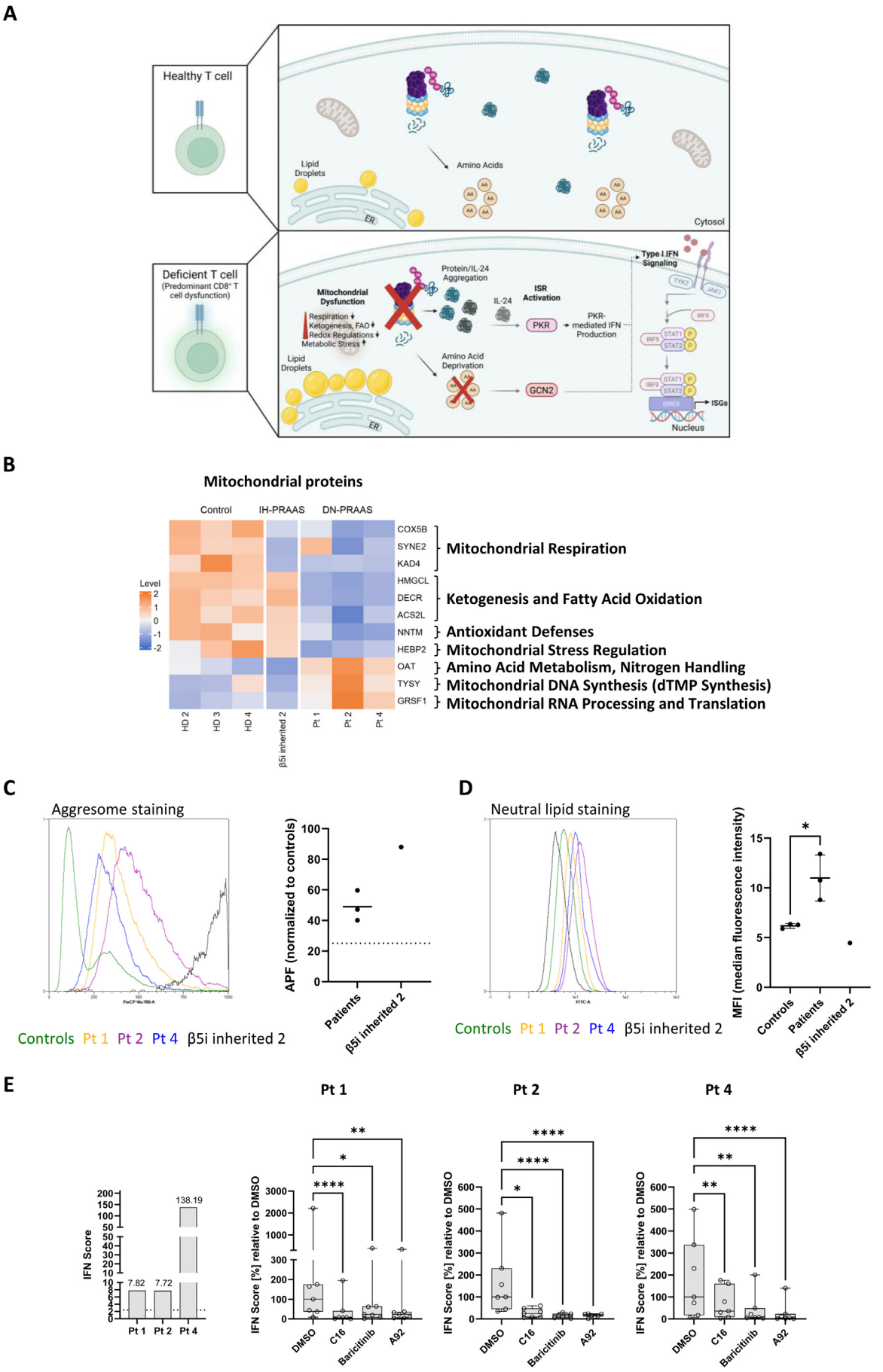

Figure 5. Molecular analysis of the patient's expanded T cells. A, Summary of affected cellular processes in deficient T cells. B, Heatmap of regulated mitochondrial proteins from proteomic profiling of patients 1, 2, and 4 (Pt 1, 2, and 4) and healthy donors (HD 2, 3, and 4), including the pathogenic variant β5i C135* homozygous (β5i inherited 2). C, Fluorescent-based protein aggregate staining assay was performed in patients' T cells (Pt 1, 2, and 4) and healthy donors (HD 1, father and mother of patient 4), including a known inherited PRAAS variant, β5i C135* (β5i inherited 2). The aggresome

ketogenesis and fatty acid oxidation (eg, HMGCL, DECR1, ACSL2), lost protective mitochondrial redox regulation (eg, NNTM and HEBP2), and upregulated proteins indicating increased amino acid metabolism and mitochondrial DNA and RNA processing (Fig 5B). These changes drive mitochondrial dysfunction that has been linked to cellular exhaustion (eg, *CTLA4* and *PDCD1*) and increased cell death (Fig S8A-B) [55]. Of note, an altered CD4/CD8 ratio of the expanded T cells for 2 patients could be observed (Fig S8C).

Protein aggregate staining confirmed disrupted proteostatic processes in both DN and biallelic PRAAS T cells compared to healthy controls (Fig 5C) with increased lysine 48 (K48)-linked ubiquitin-conjugates (Fig S9B). In addition, lipid droplet formation, a sign of impaired fatty acid utilisation and maladaptive proteotoxic stress buffering [56,57], was notably increased in DN-PRAAS T cells, but not in biallelic cases (Fig 5D). These droplets were recently found to sequester ubiquitylated proteins under stress [58], reflecting a dysfunctional response to severe cell stress.

Several cell stress pathways converge on eIF2α phosphorylation to activate the ISR [59,60]. Proteasome impairment also depletes the intracellular free amino acid pool, activating general control nonderepressible 2 (GCN2) via uncharged tRNA sensing [61]. Inhibitor studies in patient T cells confirmed that PKR inhibition (C16) and GCN2 inhibition (A92) significantly reduced IFN-I scores, comparable to the JAKi baricitinib (Fig 5E). In contrast, inhibition of an endoplasmic reticulum stress sensor, IRE1α (by 4μ8c), or of the dinucleotide sensor stimulator of interferon gene (by H-151) had no significant effect (Fig S9C). These findings highlight the increased mitochondrial, proteotoxic, and lipotoxic stress responses as central features of T cell activation in DN-PRAAS over biallelic PRAAS and suggest PKR and possibly GCN2 as potential therapeutic targets.

DISCUSSION

PRAAS comprises a spectrum of IFN-I-driven autoinflammatory disorders caused by LOF variants in 20S proteasome subunits or their assembly factors. We report a heterozygous, de novo, DN-*PSMB8* mutation, p.G209R, that expands the genophenotype associations of *PSMB8*-related CANDLE/PRAAS beyond recessive inheritance, introducing immune dysregulation and cytopenias as dominant clinical features. This variant deepens our understanding of proteasome dysfunction by integrating structural and functional modelling of progressive 20S proteasome impairment and supporting a severity-dependent disease model with novel biomarkers and implications for a personalised therapeutic approach.

Unlike the 'classic PRAAS' phenotype associated with homozygous founder mutations p.T75M and p.G201V in Hispanic [20,21] and Japanese populations [22,23], respectively, DN-*PSMB8* PRAAS manifests with immunodeficiency, T and B cell lymphopenia, perinatal infections, and vascular liver and renal involvement, resembling features of POMP-related autoinflammation and immune dysregulation [33].

The de novo *PSMB8* p.G209R variant leads to severe impairment of β5i-propeptide processing, affecting ~75% of the immunoproteasomes. Structural modelling revealed that the 'bulky', positively charged mutant arginine residue at position 209 that replaces the highly conserved wild-type glycine protrudes into the β4/β5i interface, creating steric clashes with β4-subunit residues (p.T139 and p.E166), and prevents proper propeptide maturation (Fig 4). Functional assays confirmed a block in final proteasome maturation at a POMP-retaining preholoproteasome state (Fig 3), explaining the profound dysfunction caused by the DN, disease-causing variant. These findings align with functional assays in previously reported DN variants, including truncating POMP variants that escape nonsense-mediated decay and incorporate into proteasome precursors [26,33], the DN-*PSMB9* variant, p.G156D (Fig S10) [29,30], and DN-*PSMB10* variants p.D56H and p.G201R [31,32]. AlphaFold3-based structural modelling of these variants suggested a similar mechanism of a steric hindrance due to altered charges or sizes of mutated amino acid residues, preventing late-stage proteasome maturation in published DN variants; moving forward, AlphaFold3-based structural modelling will likely improve pathogenesis predictions of novel proteasome variants and of variants of uncertain significance.

Our observations link T cell-intrinsic stress to pathomechanisms likely contributing to cytopenias and related complications, including recurrent infections and porto-sinusoidal vascular liver disease (PSVD) of the liver. While transient cytopenias (including lymphopenia and hypogammaglobulinemia) can occur in response to high levels of IFN-I and often improve with IFN-blocking therapies [62], the persistent and severe cytopenias observed in DN-PRAAS patients point to a multifactorial aetiology. Molecular profiling identifies mitochondrial and metabolic stress markers as being associated with disease severity. While intracellular protein aggregates reflect proteotoxic stress, they do not correlate with clinical phenotype. In contrast, lipid droplet accumulation and progressive upregulation of mitochondrial stress response genes offer a more reliable readout of proteotoxic, lipotoxic, and mitochondrial dysfunction, likely driving T cell exhaustion and cell death in activated cells, contributing to cytopenias and the immunodeficiency-related disease manifestations in DN-PRAAS patients, which are most pronounced during infections. Importantly, these markers also associate with clinical manifestations of immune deficiency such as viral susceptibility and liver pathology, supporting their potential for risk stratification. Proteasome dysfunction is known to disrupt the development and maintenance of medullary thymic epithelial cells (mTEC), leading to thymic hypoplasia or involution and T cell repertoire reduction and impaired central T cell tolerance [63–65]. Notably, the DN-*PSMB10* variant, p.G201R, has been associated with profound cytopenias mimicking SCID- or Omenn-like phenotypes in infants, particularly in the context of perinatal infections [31,32]. Proteasome dysfunction appears to disproportionately affect $CD8^+$ T cell repertoire development and antiviral competence [66,67], which is caused by $CD8^+$ T cells undergoing positive selection in the thymus based on cytosolic peptides processed by proteasomes and presented in a major histocompatibility complex (MHC) class I-

propensity factor (APF) was calculated for each sample using the mean of controls. D, Neutral lipid staining assay for triglycerides was used to stain patients' T cells (Pt 1, 2, and 4) and healthy donors (HD 1, father and mother of patient 4), including a known inherited PRAAS variant β5i C135* (β5i inherited 2). E, RT-qPCR analysis of 7 interferon-stimulated genes (ISGs) was performed to calculate the interferon (IFN) score of patients' expanded T cells (Pt 1, 2, and 4), including 16-hour inhibitor treatments for: PKR (5 μM C16), JAK1 (1 μM baricitinib), and GCN2 (10 μM A92). Statistical testing was applied by performing a Friedman test with Dunn's correction in GraphPad Prism (v.10.2.2). *P* value ≤0.05 (*), ≤0.01 (**), ≤0.001 (***), ≤0.0001(****). Created in BioRender. Venz, S. (2025) https://BioRender.com/9bknfxj.

restricted manner by cortical thymic epithelial cells. Disruption of this pathway reduces thymic selection efficiency and narrows the $CD8^+$ T cell repertoire [32,68]. In contrast, $CD4^+$ T cells, which are selected on antigens processed independent of the proteasome in endosomal/lysosomal compartments and presented via MHC class II, are comparatively spared [69,70]. The impact of the disease-causing variants on CD8+ and CD4+ T cell repertoire development is currently unknown, and future studies are needed to provide further insights into T cell dysfunction and repertoire restricting in contributing to the immunodeficiency phenotype of DN patients.

The divergent hepatic manifestations between PRAAS genotypes, hepatic steatosis in biallelic PRAAS and PSVD/NRH in DN-PRAAS, align with differences in mitochondrial and lipid stress. We found that the DN variant *PSMB8* p.G209R causes a more profound defect in proteasome biogenesis, leading to heightened proteotoxic and metabolic stress. This disrupts key mitochondrial pathways critical for lipid metabolism, including ketogenesis and fatty acid β-oxidation, which remain relatively preserved in the biallelic CANDLE/PRAAS patients. Consequently, DN-PRAAS patients may lack hepatic steatosis due to impaired lipid handling and oxidative stress–mediated inhibition of β-oxidation, whereas patients with homozygous PRAAS retain partial mitochondrial function and accumulate hepatic lipid stores [71,72]. Nonalcoholic fatty liver disease/nonalcoholic steatohepatitis models support this dichotomy with mild mitochondrial dysfunction promoting steatosis and severe dysfunction resulting in hepatocyte injury [73,74].

Additional factors that may exacerbate liver pathology include increased gut permeability resulting in microbial translocation [50]. This could amplify immune-mediated endothelial damage, driving PSVD, including NRH and thrombotic microangiopathy, which have been reported in inborn errors of immunity associated with cytopenias, T cell–targeted immunosuppression post-HSCT [75,76], and IFN-I–mediated immune dysregulation [77]. Notably, 4 DN-PRAAS patients developed transient but prolonged expansions of activated, cytotoxic $CD8^+$ T cells postinfection (Table S1), suggesting oligoclonal T cell activation that may contribute to sinusoidal endothelial damage and NRH, similar to what has been proposed in common variable immunodeficiency [78] and chronic granulomatous disease [79]. These findings indicate that severe proteasome assembly defects, compounded by mitochondrial and lipotoxic stress and impaired redox regulation, likely drive the collapse of hepatocyte lipid homeostasis and cytopenia-mediated endothelial and sinusoidal injury. This highlights the need for disease severity biomarkers beyond proteasome activity. Whether cell stress signatures in activated T cells can identify patients at risk for PSVD warrants further investigation.

Previous studies underscore a central role for the ISR in propagating disease [48]. PKR, a key eIF2α kinase, amplifies IFN-I signalling in response to misfolded IL-24 under proteotoxic stress, a process exacerbated by amino acid starvation [48,80–82]. Although GCN2 was not directly implicated in that study, its known activation under amino acid deprivation suggests it also contributes to the ISR signalling in PRAAS [48,83,84]. Our findings demonstrate that pharmacologic inhibition of GCN2 reduces IFN-I signalling, supporting convergence with PKR in modulating IFN output and orchestrating eIF2α-driven cell-fate transitions.

These insights may inform treatment stratification. While JAK inhibitors remain the cornerstone of treatment in PRAAS, IFNAR blockade (eg, anifrolumab) may provide added benefit in patients with incomplete responses or T cell-mediated immunodeficiencies [85]. Given the variability in HSCT outcomes across PRAAS genotypes [46], personalised treatment approaches that include rigorous management of the inflammatory disease manifestations are essential. Stress-response biomarkers may prove valuable in guiding therapy and predicting disease progression.

In summary, the *PSMB8* p.G209R variant causes a DN form of PRAAS characterised by severe immune and metabolic stress, cytopenias, and organ involvement. Structural modelling elucidates the molecular basis of its disruptive effect, while integration of genotype, functional biomarkers, and clinical features supports a continuum of mitochondrial, proteotoxic, and lipotoxic stress responses that contribute to maladaptive responses that drive disease severity. Future research should focus on dissecting tissue-specific stress pathways and exploring their therapeutic modulation. Ultimately, PRAAS provides a compelling model for investigating the intersection of proteostasis failure, maladaptive tissue stress responses, and immune dysfunction, with broader implications for immunologic, metabolic, and degenerative diseases.

Acknowledgements

We thank Prof. Dr Oliver Otto and his group, especially Doreen Biedenweg, for supporting this work with technical equipment and knowledge for single-cell sorting. We also want to thank the group of Prof. Dr. Jens Fielitz and Caterina Redwanz for providing and supervising on the device to perform the NanoString measurements, and we would like to additionally thank Prof. Dr. Lars Kaderali and his group, especially Dr. Yonatan Mekonnen, for initial support. We are grateful for the excellent technical assistance from Anne Brandenburg, Robert Beyer, and Katrin Schoknecht. We would like to thank Katherine Myint-Hpu for her assistance in bone marrow biopsies and lumbar punctures. We would like to thank Renata R. Dias for her contribution to the collection of patient data and clinical assessment of patient 3, as well as Adriana Maluf Elias and Lucia Campos for the clinical evaluation of patient 3. We thank Dr. Julien Thevenon and the 2025 French Genomic Medicine Initiative for data on patient 7 and Dr Jérémie Rosain for the genetic analysis of patient 8. We thank the patients and their families for their commitment.

Schematic illustrations were designed in BioRender.com.

Contributors

SW: Performed experiments, data interpretation, data analysis, figure design, manuscript writing, and manuscript revision. SA: Performed experiments, clinical data collection, data interpretation, data analysis, figure design, manuscript writing, and manuscript revision. MW: Bioinformatic predictions of mutations, molecular modelling, data interpretation, figure design, manuscript writing, and manuscript revision. FGT: Performed experiments, data analysis, and manuscript revision. AJ: Genetic analysis, clinical data collection, and manuscript revision. JJP: Performed experiments, data analysis, and manuscript revision. HW: Data analysis and manuscript revision. FLA: Performed experiments. EB: Performed experiments and manuscript revision. KU: Patient care, clinical data collection, and manuscript revision. FB: Clinical biomarker analysis and manuscript revision. AM: Patient data collection and manuscript revision. LS: Data analysis and manuscript revision. CH: Performed experiments and manuscript revision. SV: Methodology and manuscript revision. RAA: Data analysis and manuscript revision. LP:

Performed cell culture cultivation. C and F: Biomarker assessment and manuscript revision. FCC: Patient care, clinical data collection, and manuscript revision. IHS: Clinical data collection and interpretation and manuscript revision. SAk: Patient care, data collection and interpretation, and manuscript revision. PJM: Patient care and manuscript revision. RSA: Patient care, clinical and laboratory data collection and interpretation, and manuscript revision. PB: Patient care and manuscript revision. TCLM: Patient care, clinical data collection, and manuscript revision. MB.D and KTK: Patient care and manuscript revision. JK and YKOT: Patient care, clinical data collection, and manuscript revision. RGMB: Patient care, genetic diagnosis, and manuscript revision. KP: Patient care and manuscript revision. ACH: Patient care, clinical data collection, and manuscript revision. PBr: Biomarker analysis and interpretation and manuscript revision. PBL, JBW, and LFS: Patient care and manuscript revision. ON: Patient care, clinical data collection and interpretation, and manuscript revision. AP: Patient care, clinical data collection, and manuscript revision. GB: Patient care and manuscript revision. MT: Patient care, clinical data collection, and manuscript revision. TWJH, BF, and BN: Patient care and manuscript revision. UV: Data analysis, funding acquisition, and manuscript revision. GWES: Manuscript revision. JMB: Biomarker assessment and interpretation and manuscript revision. KRC and DK: Clinical data collection and interpretation and manuscript revision. FE: Study design, performed experiments, and manuscript revision. EK: Study design, figure design, data interpretation, manuscript writing and revision, and funding acquisition. RGM: Study design, figure design, data interpretation, manuscript writing, revision, and funding.. All authors improved and accepted the final version of the manuscript.

Funding

This work was funded by the Deutsche Forschungsgemeinschaft (DFG, German Research Foundation, 443535983; RTG 2719) and the DFG-Priority Program ‘Integration of mitochondria into the cellular proteostasis network’ (DFG SPP 2453 KR1915/11-1). This research was supported in part by the Intramural Research Program of the National Institutes of Health (NIH). RGM’s program receives intramural support ZIA AI001220. The contributions of the NIH authors were made as part of their official duties as NIH federal employees, are in compliance with agency policy requirements, and are considered Works of the United States Government. However, the findings and conclusions presented in this paper are those of the author (s) and do not necessarily reflect the views of the NIH or the U. S. Department of Health and Human Services. Additional support was provided by the I-SITE Nantes Excellence Trajectory (NExT) program (project NDD-UBIPRO). P.B. was supported by the French Foundation for Medical Research (FRM, EA20170638020), the MD-PhD program of the Imagine Institute (with the support of the Fondation Bettencourt-Schueller), and a ‘Poste CCA-INSERM-Bettencourt’ (with the support of the Fondation Bettencourt-Schueller).

Competing interests

All authors declare they have no competing interests.

Patient consent for publication

Not applicable.

Ethics approval

Please see ethics statement in materials and methods section.

Provenance and peer review

Not applicable.

Data availability statement

The proteome dataset (PXD062316) is available at the PRIDE website (http://www.ebi.ac.uk/pride). The transcriptome dataset (GSE308642) is available at the GEO website (https://www.ncbi.nlm.nih.gov/geo/).

Supplementary materials

Supplementary material associated with this article can be found in the online version at doi:10.1016/j.ard.2025.10.021.

Orcid

Sophie Wolfgramm: http://orcid.org/0009-0004-0353-6457
Sara Alehashemi: http://orcid.org/0000-0002-6531-6108
Martin Wendlandt: http://orcid.org/0009-0007-7151-3961
Franziska G. Thiel: http://orcid.org/0000-0001-6322-9222
Adriana A. de Jesus: http://orcid.org/0000-0001-8966-8362
Hannes Wolfgramm: http://orcid.org/0000-0002-6028-0046
Flavia Llorente Alvarez: http://orcid.org/0009-0007-4453-1507
Farzana Bhuyan: http://orcid.org/0000-0003-2316-1221
Leif Steil: http://orcid.org/0000-0002-0733-8421
Simone Venz: http://orcid.org/0009-0004-6544-8524
Ruba Al Abdulla: http://orcid.org/0000-0002-5194-9801
Léa Poirier: http://orcid.org/0009-0003-7400-8363
Christopher Friend: http://orcid.org/0009-0000-3277-026X
Shoghik Akoghlanian: http://orcid.org/0000-0002-8264-316X
Peter J. Mustillo: http://orcid.org/0000-0002-8420-8655
Roshini S. Abraham: http://orcid.org/0000-0001-8109-8502
Paul Bastard: http://orcid.org/0000-0002-5926-8437
Jesper Kers: http://orcid.org/0000-0002-2418-5279
Y. K. Onno Teng: http://orcid.org/0000-0001-9920-2195
Robbert G.M. Bredius: http://orcid.org/0000-0001-8151-1539
Karin Palmblad: http://orcid.org/0000-0003-1197-5201
AnnaCarin Horne: http://orcid.org/0000-0002-2878-4463
Petter Brodin: http://orcid.org/0000-0002-8103-0046
Pilar Blanco-Lobo: http://orcid.org/0000-0003-1893-8198
José Bernabeu-Wittel: http://orcid.org/0000-0002-3639-8482
Olaf Neth: http://orcid.org/0000-0001-5018-0466
Guilaine Boursier: http://orcid.org/0000-0002-2903-3135
Maud Tusseau: http://orcid.org/0009-0001-2699-3827
Thomas W.J. Huizinga: http://orcid.org/0000-0001-7033-7520
Benjamin Fournier: http://orcid.org/0000-0003-4383-7524
Bénédicte Neven: http://orcid.org/0000-0001-8941-0935
Uwe Völker: http://orcid.org/0000-0002-5689-3448
Gijs W.E. Santen: http://orcid.org/0000-0003-1959-3267
Jason M. Brenchley: http://orcid.org/0000-0001-8357-2984
Frédéric Ebstein: http://orcid.org/0000-0002-3729-7878
Elke Krüger: http://orcid.org/0000-0002-2551-242X
Raphaela Goldbach-Mansky: http://orcid.org/0000-0001-7865-5769

REFERENCES

[1] Goldbach-Mansky R, Alehashemi S, De Jesus AA. Emerging concepts and treatments in autoinflammatory interferonopathies and monogenic systemic lupus erythematosus. Nat Rev Rheumatol 2025;21:22–45. doi: 10.1038/s41584-024-01184-8.

[2] Vargas JNS, Hamasaki M, Kawabata T, Youle RJ, Yoshimori T, et al. The mechanisms and roles of selective autophagy in mammals. Nat Rev Mol Cell Biol 2023;24:167–85. doi: 10.1038/s41580-022-00542-2.

[3] Dikic I. Proteasomal and autophagic degradation systems. Annu Rev Biochem 2017;86:193–224. doi: 10.1146/annurev-biochem-061516-044908.

[4] Kwon YT, Ciechanover A. The ubiquitin code in the ubiquitin-proteasome system and autophagy. Trends Biochem Sci 2017;42:873–86. doi: 10.1016/j.tibs.2017.09.002.

[5] Enenkel C, Ernst OP. Proteasome dynamics in response to metabolic changes. Front Cell Dev Biol 2025;13. doi: 10.3389/fcell.2025.1523382.

[6] Bard JAM, Goodall EA, Greene ER, Jonsson E, Dong KC, Martin A. Structure and function of the 26S proteasome. Annu Rev Biochem 2018;87:697–724. doi: 10.1146/annurev-biochem-062917-011931.

[7] Sam PN, Avery E, Claypool SM. Proteolytic control of lipid metabolism. ACS Chem Biol 2019;14:2406–23. doi: 10.1021/acschembio.9b00695.

[8] Kodroń A, Mussulini BH, Pilecka I, Wiśniewska M, Dobrowolska A, Pałka M, et al. The ubiquitin-proteasome system and its crosstalk with mitochondria as therapeutic targets in medicine. Pharmacol Res 2021;163:105248. doi: 10.1016/j.phrs.2020.105248.

[9] Çetin G, Klafack S, Studencka-Turski M, Krüger E, Ebstein F, Dubiel W, et al. The ubiquitin–proteasome system in immune cells. Biomolecules 2021;11:60. doi: 10.3390/biom11010060.

[10] Coux O, Tanaka K, Goldberg AL. Structure and functions of the 20s and 26s proteasomes. Annu Rev Biochem 1996;65:801–47. doi: 10.1146/annurev.bi.65.070196.004101.

[11] Dahlmann B. Proteasomes. Essays Biochem 2005;41:31–48. doi: 10.1042/bse0410031.

[12] Kasahara M, Flajnik MF. Origin and evolution of the specialized forms of proteasomes involved in antigen presentation. Immunogenetics 2019;71:251–61. doi: 10.1007/s00251-019-01105-0.

[13] Groettrup M, Kirk CJ, Basler M. Proteasomes in immune cells: more than peptide producers? Nat Rev Immunol 2010;10:73–8. doi: 10.1038/nri2687.

[14] Ebstein F, Kloetzel P-M, Krüger E, Seifert U, Budeus B, Schlosser A, et al. Emerging roles of immunoproteasomes beyond MHC class I antigen processing. Cell Mol Life Sci 2012;69:2543–58. doi: 10.1007/s00018-012-0938-0.

[15] Seifert U, Bialy LP, Ebstein F, Bech-Otschir D, Voigt A, Schröter F, et al. Immunoproteasomes preserve protein homeostasis upon interferon-induced oxidative stress. Cell 2010;142:613–24. doi: 10.1016/j.cell.2010.07.036.

[16] Basler M, Groettrup M. On the role of the immunoproteasome in protein homeostasis. Cells 2021;10:3216. doi: 10.3390/cells10113216.

[17] Ebstein F, Poli Harlowe MC, Studencka-Turski M, Krüger E, Kloetzel P-M, Seifert U, et al. Contribution of the unfolded protein response (UPR) to the pathogenesis of proteasome-associated autoinflammatory syndromes (PRAAS). Front Immunol 2019;10:2756. doi: 10.3389/fimmu.2019.02756.

[18] Heink S, Ludwig D, Kloetzel P-M, Krüger E, Freitag L, Schmidt F, et al. IFN-γ-induced immune adaptation of the proteasome system is an accelerated and transient response. Proc Natl Acad Sci 2005;102:9241–6. doi: 10.1073/pnas.0501711102.

[19] Bai M, Zhao X, Sahara K, Kawano H, Tanaka K, Ichihara A, et al. Assembly mechanisms of specialized core particles of the proteasome. Biomolecules 2014;4:662–77. doi: 10.3390/biom4030662.

[20] Liu Y, Ramot Y, Torrelo A, Paller AS, Si N, Babay S, et al. Mutations in proteasome subunit β type 8 cause chronic atypical neutrophilic dermatosis with lipodystrophy and elevated temperature with evidence of genetic and phenotypic heterogeneity. Arthritis Rheum 2012;64:895–907. doi: 10.1002/art.33368.

[21] Garg A, Hernandez MD, Sousa AB, Subramanyam L, Martínez de Villarreal L, dos Santos HG, et al. An autosomal recessive syndrome of joint contractures, muscular atrophy, microcytic anemia, and panniculitis-associated lipodystrophy. J Clin Endocrinol Metab 2010;95:E58–63. doi: 10.1210/jc.2010-0488.

[22] Kitamura A, Maekawa Y, Uehara H, Izumi K, Kawachi I, Nishizawa M, et al. A mutation in the immunoproteasome subunit PSMB8 causes autoinflammation and lipodystrophy in humans. J Clin Invest 2011;121:4150–60. doi: 10.1172/JCI58414.

[23] Arima K, Kinoshita A, Mishima H, Kanazawa N, Kaneko T, Mizushima T, et al. Proteasome assembly defect due to a proteasome subunit beta type 8 (PSMB8) mutation causes the autoinflammatory disorder, Nakajo-Nishimura syndrome. Proc Natl Acad Sci 2011;108:14914–9. doi: 10.1073/pnas.1106015108.

[24] Arimochi H, Sasaki Y, Kitamura A, Yasutomo K, Nishikomori R, Nakagawa K. Dysfunctional immunoproteasomes in autoinflammatory diseases. Inflamm Regen 2016;36. doi: 10.1186/s41232-016-0011-8.

[25] Papendorf JJ, Ebstein F, Alehashemi S, Staufner C, Wolf NI, Schmickel K, et al. Identification of eight novel proteasome variants in five unrelated cases of proteasome-associated autoinflammatory syndromes (PRAAS). Front Immunol 2023;14:1190104. doi: 10.3389/fimmu.2023.1190104.

[26] Brehm A, Liu Y, Sheikh A, Marrero B, Omoyinmi E, Zhou Q, et al. Additive loss-of-function proteasome subunit mutations in CANDLE/PRAAS patients promote type I IFN production. J Clin Invest 2015;125:4196–211. doi: 10.1172/JCI81260.

[27] Sarrabay G, Méchin D, Salhi A, Bastard P, Touitou I, Jeru I, et al. PSMB10, the last immunoproteasome gene missing for PRAAS. J Allergy Clin Immunol 2020;145:1015–7 e6. doi: 10.1016/j.jaci.2019.11.024.

[28] Verhoeven D, Schonenberg-Meinema D, Ebstein F, Krüger E, van Royen-Kerkhof A, van Gijn M E, et al. Hematopoietic stem cell transplantation in a patient with proteasome-associated autoinflammatory syndrome (PRAAS). J Allergy Clin Immunol 2022;149:1120–7 e8. doi: 10.1016/j.jaci.2021.07.039.

[29] Kataoka S, Kawashima N, Okuno Y, Fujio K, Yamamoto K, Kanazawa N, et al. Successful treatment of a novel type I interferonopathy due to a de novo PSMB9 gene mutation with a Janus kinase inhibitor. J Allergy Clin Immunol 2021;148:639–44. doi: 10.1016/j.jaci.2021.03.010.

[30] Kanazawa N, Hemmi H, Kinjo N, Fujimoto N, Amano H, Ohmura K, et al. Heterozygous missense variant of the proteasome subunit β-type 9 causes neonatal-onset autoinflammation and immunodeficiency. Nat Commun 2021;12:6819. doi: 10.1038/s41467-021-27085-y.

[31] Van Der Made CI, Kersten S, Chorin O, van den Berge K, van Diemen CC, Verhoeven D, et al. Expanding the PRAAS spectrum: de novo mutations of immunoproteasome subunit β-type 10 in six infants with SCID-Omenn syndrome. Am J Hum Genet 2024;111:791–804. doi: 10.1016/j.ajhg.2024.02.013.

[32] Kuehn HS, Bosticardo M, Arrieta AC, van der Made CI, Oliveira JB, Notarangelo LD, et al. Thymic and T-cell intrinsic critical roles associated with severe combined immunodeficiency and Omenn syndrome due to a heterozygous variant (G201R) in PSMB10. J Allergy Clin Immunol 2025;155:1378–85 e2. doi: 10.1016/j.jaci.2024.12.1082.

[33] Poli MC, Ebstein F, Nicholas SK, de Guzman MM, Forbes LR, Chinn IK, et al. Heterozygous truncating variants in POMP escape nonsense-mediated decay and cause a unique immune dysregulatory syndrome. Am J Hum Genet 2018;102:1126–42. doi: 10.1016/j.ajhg.2018.04.010.

[34] De Jesus AA, Brehm A, VanTries R, Pillet P, Parentelli AS, Sanchez GAM, et al. Novel proteasome assembly chaperone mutations in *PSMG2*/PAC2 cause the autoinflammatory interferonopathy CANDLE/PRAAS4. J Allergy Clin Immunol 2019;143:1939–43 e8. doi: 10.1016/j.jaci.2018.12.1012.

[35] Meinhardt A, Ramos PC, Dohmen RJ, Jansen NS, Lankester AC, Ebstein F, et al. Curative treatment of POMP-related autoinflammation and immune dysregulation (PRAID) by hematopoietic stem cell transplantation. J Clin Immunol 2021;41:1664–7. doi: 10.1007/s10875-021-01067-7.

[36] Cavalcante MPV, Brunelli JB, Miranda CC, Fonseca EOL, da Rocha Sobrinho HM, Magalhães T, et al. CANDLE syndrome: chronic atypical neutrophilic dermatosis with lipodystrophy and elevated temperature—a rare case with a novel mutation. Eur J Pediatr 2016;175:735–40. doi: 10.1007/s00431-015-2668-4.

[37] McDermott A, Jesus AA, Liu Y, Kim P, Jacks J, Sanchez GAM, et al. A case of proteasome-associated auto-inflammatory syndrome with compound heterozygous mutations in PSMB8. J Am Acad Dermatol 2013;69:e29–32. doi: 10.1016/j.jaad.2013.01.015.

[38] Jia T, Zheng Y, Feng C, Yang J, Zhang J, Li C, et al. A Chinese case of Nakajo–Nishimura syndrome with novel compound heterozygous mutations of the PSMB8 gene. BMC Med Genet 2020;21:126. doi: 10.1186/s12881-020-01060-8.

[39] Contreras-Cubas C, Cárdenas-Conejo A, Rodríguez-Velasco A, Gómez-Díaz B, Gómez-Ruiz C, Córdova EJ, et al. A homozygous mutation in the *PSMB8* gene in a case with proteasome-associated autoinflammatory syndrome. Scand J Rheumatol 2018;47:251–4. doi: 10.1080/03009742.2017.1342273.

[40] Boyadzhiev M, Marinov L, Boyadzhiev V, Iliev E, Stefanova P, Ivanov I, et al. Disease course and treatment effects of a JAK inhibitor in a patient with CANDLE syndrome. Pediatr Rheumatol 2019;17:19. doi: 10.1186/s12969-019-0322-9.

[41] Agarwal AK, Xing C, DeMartino GN, Mizrachi D, Hernandez MD, Sousa AB, et al. *PSMB8* encoding the β5i proteasome subunit is mutated in joint contractures, muscle atrophy, microcytic anemia, and panniculitis-induced lipodystrophy syndrome. Am J Hum Genet 2010;87:866–72. doi: 10.1016/j.ajhg.2010.10.031.

[42] Yamazaki-Nakashimada MA, Santos-Chávez EE, de Jesus AA, Ramírez-Vargas N, Alarcón-Segovia D, Orozco L, et al. Systemic autoimmunity in a patient with CANDLE syndrome. J Investig Allergol Clin Immunol 2019;29:75–6. doi: 10.18176/jiaci.0338.

[43] Patel PN, Hunt R, Pettigrew ZJ, Al Hammadi R, McEwen FS, Wilson N, et al. Successful treatment of chronic atypical neutrophilic dermatosis with

lipodystrophy and elevated temperature (CANDLE) syndrome with tofacitinib. Pediatr Dermatol 2021;38:528–9. doi: 10.1111/pde.14517.
[44] Kluk J, Rustin M, Brogan PA, Lachmann HJ, Eleftheriou D, Omoyinmi E, et al. Chronic atypical neutrophilic dermatosis with lipodystrophy and elevated temperature syndrome: a report of a novel mutation and review of the literature. Br J Dermatol 2014;170:215–7. doi: 10.1111/bjd.12600.
[45] Miyamoto T, Honda Y, Izawa K, Yoshida M, Kawai T, Nishikomori R, et al. Assessment of type I interferon signatures in undifferentiated inflammatory diseases: a Japanese multicenter experience. Front Immunol 2022; 13:905960. doi: 10.3389/fimmu.2022.905960.
[46] Zhang J, Tao P, Deuitch NT, Liu Y, Goldbach-Mansky R, Brogan PA, et al. Proteasome-associated syndromes: updates on genetics, clinical manifestations, pathogenesis, and treatment. J Clin Immunol 2024;44:88. doi: 10.1007/s10875-024-01692-y.
[47] Sanchez GAM, Reinhardt A, Ramsey S, Wittkowski H, Hashkes PJ, Berkun Y, et al. JAK1/2 inhibition with baricitinib in the treatment of autoinflammatory interferonopathies. J Clin Invest 2018;128:3041–52. doi: 10.1172/JCI98814.
[48] Davidson S, Yu C-H, Steiner A, Ebstein F, Sedghi M, Nicchitta C, et al. Protein kinase R is an innate immune sensor of proteotoxic stress via accumulation of cytoplasmic IL-24. Sci Immunol 2022;7:eabi6763. doi: 10.1126/sciimmunol.abi6763.
[49] Isidor B, Ebstein F, Hurst A, Pasquier L, Bézieau S, Thevenon J, et al. Stankiewicz-Isidor syndrome: expanding the clinical and molecular phenotype. Genet Med 2022;24:179–91. doi: 10.1016/j.gim.2021.09.005.
[50] Llorente C, Schnabl B. The gut microbiota and liver disease. Cell Mol Gastroenterol *Hepatol* 2015;1:275–84. doi: 10.1016/j.jcmgh.2015.04.003.
[51] Adolf F, Du J, Goodall EA, van der Lee R, Ben-Nissan G, Guo X, et al. Visualizing chaperone-mediated multistep assembly of the human 20S proteasome. Nat Struct Mol Biol 2024;31:1176–88. doi: 10.1038/s41594-024-01268-9.
[52] Ramos PC, Marques AJ, London MK, Dohmen RJ. Role of C-terminal extensions of subunits β2 and β7 in assembly and activity of eukaryotic proteasomes. J Biol Chem 2004;279:14323–30. doi: 10.1074/jbc.M308757200.
[53] Huber EM, Heinemeyer W, Li X, Arendt CS, Hochstrasser M, Groll M. A unified mechanism for proteolysis and autocatalytic activation in the 20S proteasome. Nat Commun 2016;7:10900. doi: 10.1038/ncomms10900.
[54] Ross J, Olson L, Coppotelli G. Mitochondrial and ubiquitin proteasome system dysfunction in ageing and disease: two sides of the same coin? Int J Mol Sci 2015;16:19458–76. doi: 10.3390/ijms160819458.
[55] Wu H, Zhao X, Hochrein SM, Dülmen M, Gao X, Yin J, et al. Mitochondrial dysfunction promotes the transition of precursor to terminally exhausted T cells through HIF-1α-mediated glycolytic reprogramming. Nat Commun 2023;14. doi: 10.1038/s41467-023-42634-3.
[56] Meçe O, Houbaert D, Sassano M-L, De Decker M, de Waele J, Eelen G, et al. Lipid droplet degradation by autophagy connects mitochondria metabolism to Prox1-driven expression of lymphatic genes and lymphangiogenesis. Nat Commun 2022;13. doi: 10.1038/s41467-022-30490-6.
[57] Geltinger F, Schartel L, Wiederstein M, Tevini J, Stelzer L, Jungwirth H, et al. Friend or foe: lipid droplets as organelles for protein and lipid storage in cellular stress response, aging and disease. Molecules 2020;25:5053. doi: 10.3390/molecules25215053.
[58] Kumar AV, Mills J, Parker WM, Lu Y, Harnett B, Babcock DT, et al. Lipid droplets modulate proteostasis, SQST-1/SQSTM1 dynamics, and lifespan in C. elegans. iScience. 2023;26:107960. doi: 10.1016/j.isci.2023.107960
[59] Acosta-Alvear D. Common signaling principles and interconnectivity in the ISR-UPR networks. FASEB J 2022;36. doi: 10.1096/fasebj.2022.36.s1.0i138.
[60] Pakos-Zebrucka K, Koryga I, Mnich K, Ljujic M, Samali A, Gorman AM. The integrated stress response. EMBO Rep 2016;17:1374–95. doi: 10.15252/embr.201642195.
[61] Wek SA, Zhu S, Wek RC. The histidyl-tRNA synthetase-related sequence in the eIF-2α protein kinase GCN2 interacts with tRNA and is required for activation in response to starvation for different amino acids. Mol Cell Biol 1995;15:4497–506. doi: 10.1128/mcb.15.8.4497.
[62] Fischer S, Proschmann U, Akgün K, Ziemssen T. Lymphocyte counts and multiple sclerosis therapeutics: between mechanisms of action and treatment-limiting side effects. Cells 2021;10:3177. doi: 10.3390/cells10113177.
[63] Murata S, Takahama Y, Kasahara M, Tanaka K. The immunoproteasome and thymoproteasome: functions, evolution and human disease. Nat Immunol 2018;19:923–31. doi: 10.1038/s41590-018-0186-z.
[64] Matsuda-Lennikov M, Ohigashi I, Takahama Y. Tissue-specific proteasomes in generation of MHC class I peptides and CD8+ T cells. Curr Opin Immunol 2022;77:102217. doi: 10.1016/j.coi.2022.102217.
[65] Yamaguchi N, Takakura Y, Akiyama T. Autophagy and proteasomes in thymic epithelial cells: essential bulk protein degradation systems for immune homeostasis maintenance. Front Immunol 2024;15. doi: 10.3389/fimmu.2024.1488020.
[66] Schmidt ME, Varga SM. The CD8 T cell response to respiratory virus infections. Front Immunol 2018;9. doi: 10.3389/fimmu.2018.00678.
[67] Cai Q, Chen K, Young KH. Epstein–Barr virus-positive T/NK-cell lymphoproliferative disorders. Exp Mol Med 2015;47 e133-e133. doi: 10.1038/emm.2014.105.
[68] Frantzeskakis M, Takahama Y, Ohigashi I. The role of proteasomes in the thymus. Front Immunol 2021;12. doi: 10.3389/fimmu.2021.646209.
[69] Klein L, Kyewski B, Allen PM, Hogquist KA. Positive and negative selection of the T cell repertoire: what thymocytes see (and don't see). Nat Rev Immunol 2014;14:377–91. doi: 10.1038/nri3667.
[70] Wu C, Aichinger M, Nedjic J, Klein L. Thymic epithelial cells use macroautophagy to turn their inside out for CD4 T cell tolerance. Autophagy 2013;9:931–2. doi: 10.4161/auto.24374.
[71] Wei Y, Rector RS, Thyfault JP, Ibdah JA. Nonalcoholic fatty liver disease and mitochondrial dysfunction. World J Gastroenterol 2008;14:193. doi: 10.3748/wjg.14.193.
[72] Das D, Paul A, Lahiri A, Chakraborty S, Bhattacharjee P, Ghosh S. Proteasome dysfunction under compromised redox metabolism dictates liver injury in NASH through ASK1/PPARγ binodal complementary modules. Redox Biol 2021;45:102043. doi: 10.1016/j.redox.2021.102043.
[73] Pecoraro A, Crescenzi L, Varricchi G, Marano L, Spadaro G, Triggiani M. Heterogeneity of liver disease in common variable immunodeficiency disorders. Front Immunol 2020;11. doi: 10.3389/fimmu.2020.00338.
[74] Fuss IJ, Friend J, Yang Z, et al. Nodular regenerative hyperplasia in common variable immunodeficiency. J Clin Immunol 2013;33:748–58. doi: 10.1007/s10875-013-9873-6.
[75] Elfeky R, Lucchini G, Lum S-H, Dvorak CC, Veys P, Amrolia PJ. New insights into risk factors for transplant-associated thrombotic microangiopathy in pediatric HSCT. Blood Adv 2020;4:2418–29. doi: 10.1182/bloodadvances.2019001315.
[76] Riller Q, Fourgeaud J, Bruneau J, Melotti A, Thomas C, Neven B. Late-onset enteric virus infection associated with hepatitis (EVAH) in transplanted SCID patients. J Allergy Clin Immunol 2023;151:1634–45. doi: 10.1016/j.jaci.2022.12.822.
[77] Tydén H, Lood C, Gullstrand B, Jönsen A, Leanderson T, Bengtsson AA. Endothelial dysfunction is associated with activation of the type I interferon system and platelets in patients with systemic lupus erythematosus. RMD Open 2017;3:e000508. doi: 10.1136/rmdopen-2017-000508.
[78] Daza-Cajigal V, Segura-Guerrero M, López-Cueto M, García-García E, Martínez-Banaclocha H, Campos-Caro A. Clinical manifestations and approach to the management of patients with common variable immunodeficiency and liver disease. Front Immunol 2023;14:1197361. doi: 10.3389/fimmu.2023.1197361.
[79] Feld JJ, Hussain N, Wright EC, Mistry N, Lee DY, Markowitz J. Hepatic involvement and portal hypertension predict mortality in chronic granulomatous disease. Gastroenterology 2008;134:1917–26. doi: 10.1053/j.gastro.2008.02.081.
[80] Ebstein F, Küry S, Most V, Syrbe S, Wiemann M, Fehling HJ. PSMC3 proteasome subunit variants are associated with neurodevelopmental delay and type I interferon production. Sci Transl Med 2023;15:eabo3189. doi: 10.1126/scitranslmed.abo3189.
[81] Deb W, Rosenfelt C, Vignard V, Girard S, Laflamme N, Roux-Dalvai F, et al. PSMD11 loss-of-function variants correlate with a neurobehavioral phenotype, obesity, and increased interferon response. Am J Hum Genet 2024;111:1352–69. doi: 10.1016/j.ajhg.2024.05.016.
[82] Küry S, Stanton JE, Van Woerden G, Kichler S, Morel A, Houge G, et al. Unveiling the crucial neuronal role of the proteasomal ATPase subunit gene PSMC5 in neurodevelopmental proteasomopathies. 2024.
[83] Suraweera A, Münch C, Hanssum A, Bertolotti A. Failure of amino acid homeostasis causes cell death following proteasome inhibition. Mol Cell 2012;48:242–53. doi: 10.1016/j.molcel.2012.08.003.
[84] Zhao C, Guo H, Hou Y, Zhang H, Wang Y, Zhang J, et al. Multiple roles of the stress sensor GCN2 in immune cells. Int J Mol Sci 2023;24:4285. doi: 10.3390/ijms24054285.
[85] Cetin Gedik K, Ortega-Villa AM, Materne G, Ombrello MJ, Zavialov AV, Biancotto A, et al. Disease flares with baricitinib dose reductions and development of flare criteria in patients with CANDLE/PRAAS. Ann Rheum Dis 2024;83:1181–8. doi: 10.1136/ard-2023-225463.